Binary Phase Behavior of 1,3-Distearoyl-2-oleoyl-*sn*-glycerol (SOS) and 1,3-Distearoyl-2-linoleoyl-*sn*-glycerol (SLS)

M. Takeuchi[a], S. Ueno[a], E. Flöter[b], and K. Sato[a,*]

[a]Faculty of Applied Biological Science, Hiroshima University, Higashi-Hiroshima 739-8528, Japan, and [b]Vlaardingen Laboratory, Unilever Research, 3133 AT Vlaardingen, The Netherlands

ABSTRACT: The binary phase behavior of SOS (1,3-distearoyl-2-oleoyl-*sn*-glycerol) and SLS (1,3-distearoyl-2-linoleoyl-*sn*-glycerol) was examined by using DSC and conventional and synchrotron radiation X-ray diffraction. The solid-solution phases were observed in the metastable α and γ forms in all concentration ranges. Results indicated that the miscible γ form did not transform to the β′ form when the mixtures were subjected to simple cooling from a high-temperature liquid to a low-temperature solid phase. However, an α-melt-mediated transformation into β′ and β_2 resulted in the formation of immiscible phases in concentration ranges of SLS below 30%. By contrast, at SLS concentration ranges above 30%, the α-melt-mediated transformation caused crystallization of only the γ form, and β′ and β_2 crystals did not appear. These results show that the specific interactions between SOS and SLS are operative in the phase behavior of the mixture states of SOS and SLS.

Paper no. J10094 in *JAOCS 79,* 627–632 (July 2002).

KEY WORDS: Binary phase behavior, 1,3-distearoyl-2-linoleoyl-*sn*-glycerol, 1,3-distearoyl-2-oleoyl-*sn*-glycerol, molecular interaction, polymorphism.

The phase behavior of TAG mixtures is one of the major factors that determines the macroscopic properties of fat products, such as mouthfeel, appearance, and rheology, together with fat polymorphism, crystal size, morphology, and crystal network formation (1–8).

Real fat systems of both vegetable and animal origin are multicomponent systems containing different kinds of FA moieties. The complex features of real fat systems are due to fat polymorphism as well as the mixing behavior of different TAG. The physical analysis of real fat systems usually starts with understanding the individual TAG molecules and subsequently moves on to understanding the mixed systems. The best approach for the latter task usually starts with studying binary mixture systems of different TAG and extends to ternary and multicomponent mixture systems. Therefore, many studies of binary phase behavior have been performed for different combinations of TAG mixtures (9–15).

In the phase behavior of binary mixture systems, three typical phases can occur: a solid-solution phase, a eutectic phase, and molecular compound formation. The general tendency in the relationship between molecular interactions and phase behavior may be summarized as follows: (i) The two components (A and B) can exchange places with one another in the crystal lattice in all concentration ratios (solid-solution phase); (ii) no solubilities will exist in the lattices of crystals A and B, respectively (eutectic phase); and (iii) highly specific interactions can give rise to the formation of molecular compounds. In the particular case of the mixture of tristearin/tripalmitin (SSS/PPP) (16,17), metastable α and β′ forms were shown to exhibit continuous solid solutions, yet a eutectic nature was revealed in the most stable β form. For PPP/1,3-dipalmitoyl-2-oleoyl-*sn*-glycerol (POP) mixtures (18,19), eutectic phases were observed in the metastable α and β′ forms and in the most stable β form as well. Recent studies on phase behavior have revealed various types of binary mixtures of TAG that form molecular compounds: 1,3-distearoyl-2-oleoyl-*sn*-glycerol/1,2-distearoyl-3-oleoyl-*rac* glycerol (SOS/SSO) (20), 1,3-distearoyl-2-oleoyl-*sn*-glycerol/1,3-dioleoyl-2-stearoyl-*sn*-glycerol (SOS/OSO) (21), 1,3-dipalmitoyl-2-oleoyl-*sn*-glycerol/1,2-dipalmitoyl-3-oleoyl-*rac*-glycerol (POP/PPO) (19,22,23), and 1,3-dipalmitoyl-2-oleoyl-*sn*-glycerol/1,3-dioleoyl-2-palmitoyl-*sn*-glycerol (POP/OPO) (19,23,24). Mechanistic considerations concerning the formation of the molecular compound in these TAG mixtures in terms of chain–chain interactions between the component TAG molecules are given elsewhere (25,26).

In the present work, we examined the binary phase behavior of SOS and 1,3-distearoyl-2-linoleoyl-*sn*-glycerol (SLS) with an emphasis on polymorphic behavior and transformation in the mixtures. The distribution of the mono- and polyunsaturated FA in the *sn*-2 position in TAG containing one or two saturated FA at the *sn*-1 and *sn*-3 positions strongly influences the properties of the saturated–unsaturated–saturated TAG (27,28). It is important to understand the physical properties of the binary mixture phases of SOS and SLS, since this mixing behavior is closely related to fat blending in fat technology and the separation of fats and oils in industrial crystallization processes. The thermal and structural properties of SOS (29–31) and SLS (32) are summarized in Table 1. SOS has five polymorphic forms—α, γ, β′, and two β forms—and SLS has two forms—α and γ. As for the α and γ forms, the physicochemical properties of SOS are similar to those of SLS. The peculiarity in the polymorphic behavior of SLS is the absence of β′ and β forms, which are present in most instances of TAG crystalline polymorphism (7,15,32). Therefore, it is interesting to observe how the polymorphic properties

*To whom correspondence should be addressed.
E-mail: kyosato@hiroshima-u.ac.jp.

TABLE 1
Thermal and Structural Properties of Polymorphic Forms of SOS (ref. 14) and SLS (ref. 15)[a]

	SOS					SLS	
	α	γ	β′	β_2	β_1	α	γ
T_m (°C)	23.5	35.4	36.5	41.0	43.0	20.8	35.0
ΔH_m (kJ/mol)	47.7	98.5	104.8	143.0	151.0	40.9	137.2
ΔS_m (J/mol/K)	160.8	319.2	338.5	455.2	477.6	139.2	445.2
LS (nm)	4.8	7.1	7.0	6.5	6.5	5.4	7.3
SS (nm)	0.421	0.472	0.424	0.458	0.458	0.412	0.474
		0.450	0.390	0.367	0.365		0.450
		0.388					0.381

[a]SOS, 1,3-distearoyl-2-oleoyl-*sn*-glycerol; SLS, 1,3-distearoyl-2-linoleoyl-*sn*-glycerol; T_m, melting point; ΔH_m, enthalpy of melting; ΔS_m, entropy of melting; LS, long-spacing value; SS, short-spacing value.

of SOS and SLS influence the phase behavior of SOS/SLS mixtures during crystallization and transformation.

EXPERIMENTAL PROCEDURES

Materials and methods. SOS was purchased from Sigma Chemical Co. (St. Louis, MO) at 99% purity. SLS was provided by Unilever Research Laboratory (Vlaardingen, The Netherlands) with purity higher than 97%. No further purification was carried out. The binary mixtures of SOS and SLS were prepared by mixing the weighed samples at room temperature, melting them above 60°C, and then rapidly cooling to 0°C. The samples were discarded after a single use to avoid the effects of oxidation.

The phase behavior of the mixtures was investigated by using DSC and two types of X-ray diffraction (XRD) generators: a conventional rotator-anode generator and a synchrotron radiation generator (as discussed below). The DSC experiments (DSC-8240; Rigaku, Tokyo Japan) were performed using the following thermal treatment. The liquid samples were cooled to –20°C at a rate of 20°C/min and maintained at that temperature for 10 min. Subsequently, the samples were heated at a rate of 2°C/min.

The XRD spectra were taken through α-melt-mediated transformation using the following thermal processes. The liquid was quenched to 10°C at a rate of 20°C/min to crystallize the α form, and after 3 min temperature was increased quickly to 30 or 36°C so that the α form melted and crystallization of the more stable forms was induced *via* the melt (α-melt mediation) (33–35). To determine the α-melt mediation at 30°C, time-resolved synchrotron radiation X-ray diffraction (SR-XRD) was used at the Photon Factory of the national Laboratory for High-Energy Physics, Tsukuba, Japan. The Photon Factory generator operates at 2.5 GeV, λ = 0.15 nm. The X-ray diffraction spectra were recorded every 10 s with two gas-filled one-dimensional position-sensitive detectors. One detector was used for the small-angle region (Rigaku; 512 channels over a total length of 200 mm), and the other was used for the wide-angle region (MAC Science, Tokyo; 512 channels over a total length of 50 mm). The distance between the sample and the detector was 1280 mm for the small-angle region and 280 mm for the wide-angle region. At 36°C, an *in situ* rotator-anode XRD (RA-XRD, λ = 0.1542 nm; Rigaku RINT-TTR) was used for α-melt mediation since it proceeded rather slowly compared to the same transformation at 30°C. In addition, the *in situ* RA-XRD spectra were taken during γ-melt-mediated crystallization by first crystallizing the γ form by quenching the liquid mixture from 60 to 25°C and then rapidly heating the γ form to 36°C to stimulate and observe the formation of more stable forms.

RESULTS

Figure 1 shows the DSC heating thermograms (0 to 50°C) of the SOS/SLS mixtures at various concentration ratios. Pure SOS showed a small endothermic peak at 23.5°C, which was soon followed by an exothermic peak around 25°C. These two peaks corresponded to the melting of the α form and

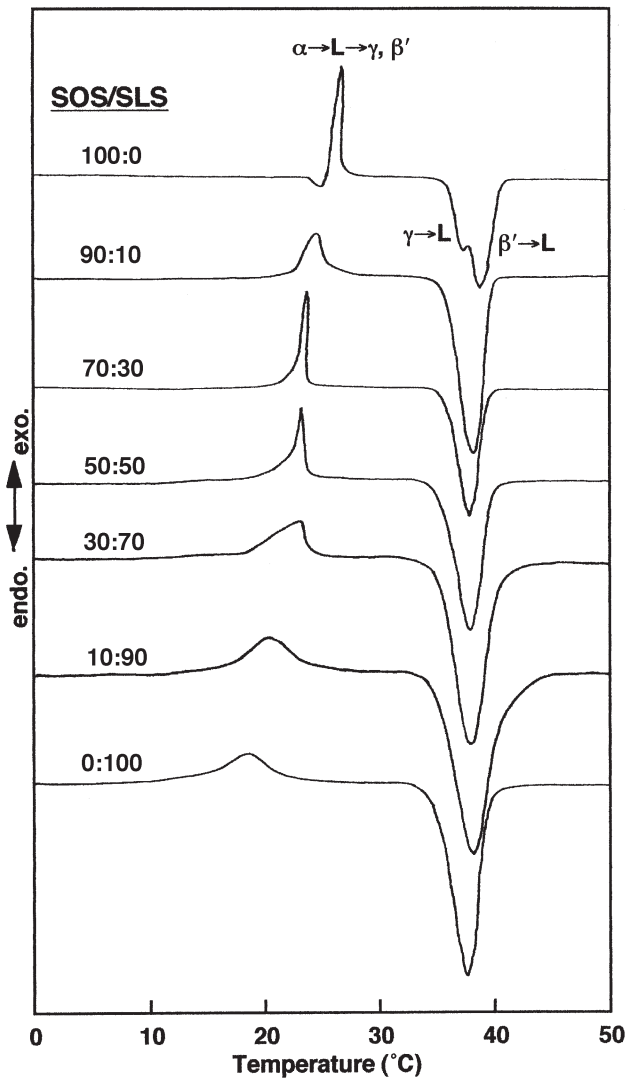

FIG. 1. DSC heating thermograms of 1,3-distearoyl-2-oleoyl-*sn*-glycerol/1,3-distearoyl-2-linoleoyl-*sn*-glycerol (SOS/SLS) mixtures at a rate of 2°C/min. L, liquid state; endo., endothermic; exo., exothermic.

rapid crystallization of the more stable γ and β′ forms. Further heating showed two overlapping endothermic peaks at 35.4 and 36.5°C, which were due to the melting of the γ and β′ forms, respectively. By contrast, the SOS/SLS mixtures showed exothermic peaks at 16–24°C and endothermic peaks at around 35°C. The former peaks correspond to the solid-state transformation from α to γ forms and the latter peaks to the melting of the γ form. From the DSC experiments shown in Figure 1, it was concluded that the SOS/SLS mixtures transformed from α to γ with no passage through the liquid state. Namely, transformation from α to γ occurred in the solid state in the SOS/SLS mixtures at the heating rate of 2°C/min. Figure 2 shows a phase diagram of the SOS/SLS binary mixtures constructed from the transformation and melting temperatures displayed in Figure 1. This phase diagram exhibits the following two points: (i) The solid-solution phases were formed in α and γ forms of the SOS/SLS mixture in the entire range of concentrations. (ii) Whereas γ to β′ transformation occurred in the pure SOS, the γ form of the mixtures did not transform to the β′ form.

The polymorphic behavior of the 75:25 SOS/SLS mixture during α-melt-mediated transformation at 30°C was monitored with time-resolved small- and wide-angle SR-XRD spectra, as shown in Figure 3. The variation of temperature applied to this SR-XRD study was as follows (see the inserted temperature–time profile in Fig. 3): The liquid mixture was chilled at 10°C and rapidly heated to 30°C so that the first occurring α crystals transformed to more stable γ and β′ forms through the α-melt transition. As shown in SR-XRD spectral changes with time–temperature variations, soon after 10°C was reached, two peaks appeared in the small-angle region, with long-spacing spectra of 5.20 (001 reflection) and 2.60 nm (002 reflection). Correspondingly, a short-spacing spectrum of 0.421 nm appeared at 10°C in the wide-angle region. These spectra showed that the α form of the SOS/SLS mixture was formed in the solid-solution phase. The temperature increase from 10 to 30°C induced melting of the α form, as shown by the disappearance of the small- and wide-angle diffraction spectra. Immediately after the α form was melted, new forms appeared having two long-spacing spectra of 7.00 (001 reflection) and 3.50 nm (002 reflection) and a sharp spectrum of 3.67 nm (002 reflection). At the same time, many short-spacing spectra appeared in the wide-angle region. The two long-spacing spectra of 7.00 and 3.50 nm were due to the β′ form of the SOS fraction, associated with the short-spacing spectra of 0.424 and 0.390 nm in the wide-angle region. On the other hand, the long-spacing spectrum of 3.67 nm and the short-spacing spectrum of 0.472 nm corresponded to the γ form of the SOS/SLS mixture. The same results were observed for SOS/SLS mixtures in the concentration range of SLS below 30%.

By contrast, no β′ form occurred in the α-melt-mediated transformation when the SLS concentration increased above 30%. Figure 4 shows the time-resolved SR-XRD spectra of the 70:30 SOS/SLS mixture during the α-melt-mediated transformation at 30°C. In this case, the single short-spacing

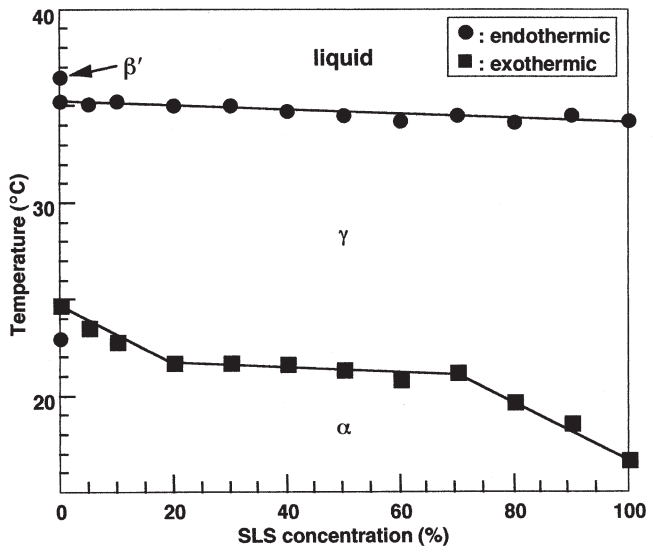

FIG. 2. Kinetic phase diagram constructed by DSC heating thermograms after quenching at a rate of 20°C/min.

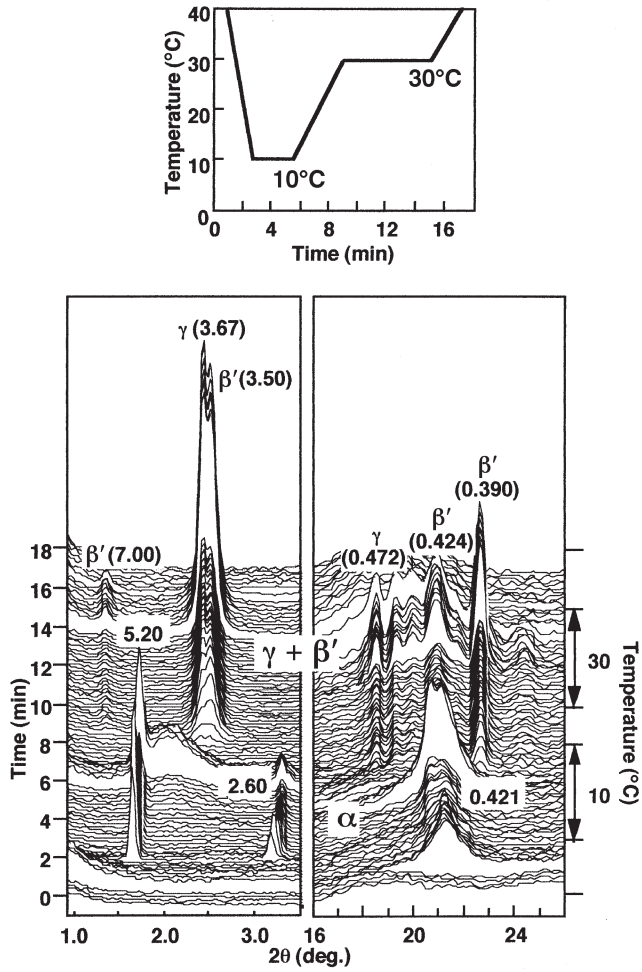

FIG. 3. Time-resolved synchrotron radiation X-ray diffraction spectra of α-melt mediation of a 75:25 SOS/SLS mixture at 10 and 30°C (temperature variation profile is inserted; unit: nm). See Figure 1 for abbreviations.

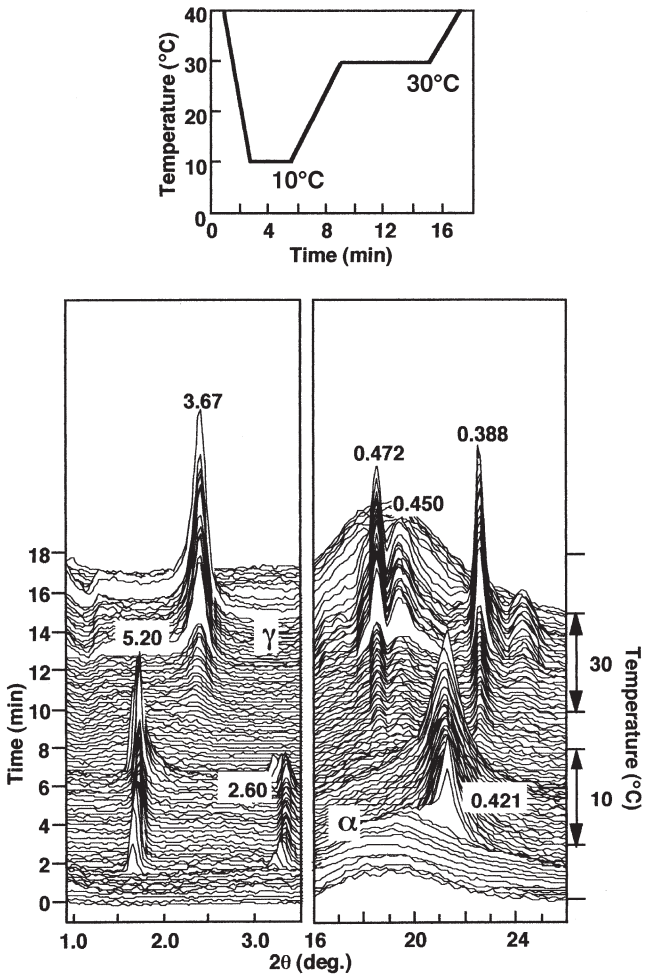

FIG. 4. Time-resolved synchrotron radiation X-ray diffraction spectra of α-melt mediation of a 70:30 SOS/SLS mixture at 10 and 30°C (temperature variation profile is inserted; unit: nm). See Figure 1 for abbreviations.

spectrum of the α form (0.421 nm) occurred together with the long-spacing spectra of 5.20 and 2.60 nm at 10°C after the quenching. By rapidly increasing the temperature to 30°C, the long- and short-spacings of the α form disappeared, and the long- (3.60 nm) and short-spacing spectra (0.472, 0.450, and 0.388 nm) of the γ form appeared, yet no β′ crystals were obtained. This indicates that the increase in the SLS concentration may have prohibited the occurrence of the β′ form in the SOS/SLS mixture during α-melt mediation.

Figure 5 shows results of the RA-XRD study of the α-melt-mediated transformation of SOS, SOS/SLS mixtures (75:25 and 70:30), and SLS when the α form was rapidly heated from 10 to 36°C. In the 75:25 SOS/SLS mixture, the β_2 form of the SOS fraction crystallized immediately, and the SLS fraction melted together with a small amount of the SOS fraction. The same result was observed in the pure SOS. However, the 70:30 SOS/SLS mixture did not crystallize in the β_2 form after the α-melt mediation at 36°C with the incubation time of about 8 h. The results of Figure 5 indicate the influence of the concentration ratio of SOS and SLS on the separation of the mixture phase during α-melt-mediation.

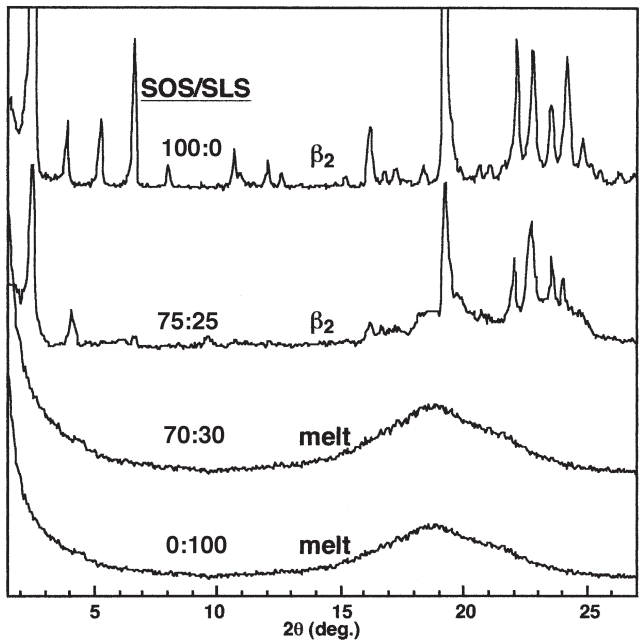

FIG. 5. *In situ* X-ray diffraction spectra of α-melt mediation of SOS/SLS mixtures at 36°C. See Figure 1 for abbreviations.

We examined the polymorphic behavior of the SOS/SLS mixture during the α-melt-mediated transformation that was carried out at different temperatures. It was found that the occurrence of γ, β′, and β_2 forms was confirmed in concentration ranges of SLS below 30%. This indicates the occurrence of separation of the SOS and SLS fractions in these concentration ranges. By contrast, above the 30% SLS concentration, we observed the crystallization of only the γ form; the β′ and β_2 forms did not crystallize. This result shows that the γ form of the SOS/SLS mixture forms a solid-solution phase and that specific interactions between the SOS and SLS fractions are operative in the γ form.

Finally, the polymorphic behavior of the SOS/SLS mixture during γ-melt-mediated transformation was studied by *in situ* RA-XRD measurement, as shown in Figure 6. The variation of temperature applied in the RA-XRD study was the following: The liquid mixture was chilled to 25°C to crystallize in the γ form and rapidly heated to 36°C. When small quantities of SLS were present in the SOS/SLS mixtures, no long- and short-spacing spectra were obtained, indicating the melting of the entire SOS/SLS mixture at 36°C. As for pure SOS, a temperature increase to 36°C immediately initiated β′ crystallization. These results show that the SLS fraction disturbs the transformation of the SOS fraction from the γ to the β′ form during γ-melt mediation.

DISCUSSION

The present experiments using DSC, SR-XRD, and RA-XRD have shown the following properties of binary phase behavior for SOS and SLS: (i) Simple cooling from a high-temperature liquid mixture that was crystallized in the α form trans-

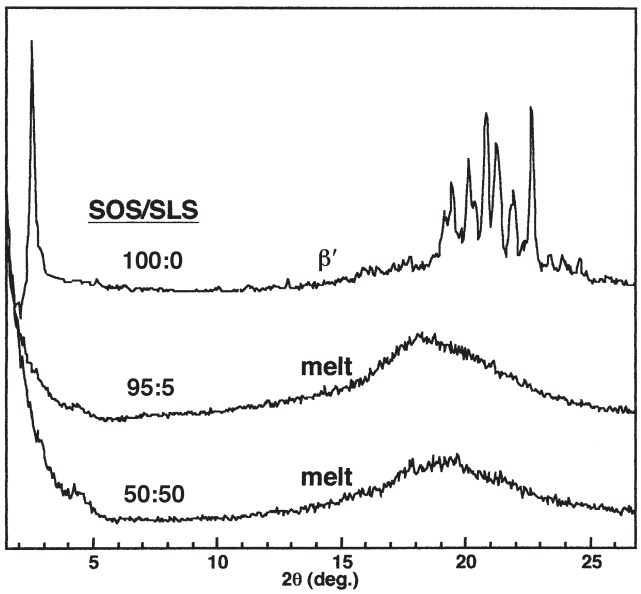

FIG. 6. *In situ* X-ray diffraction spectra of γ-melt mediation of SOS/SLS mixtures at 36°C. See Figure 1 for abbreviations.

formed it to the γ form. (ii) The α and γ forms revealed miscibility at all concentrations of SOS and SLS. (iii) In mixtures with SLS concentrations lower than 30%, α-melt- and γ-melt-mediated transformations caused phase separation of the SOS fraction, which was crystallized in β′ (at 30°C) and β_2 (at 36°C) forms. (iv) In mixtures containing SLS above a 30% concentration, no phase separation or transformation to the β′ occurred through α-melt-mediation.

The above results indicate the strong influence of chain–chain interactions between the SOS and SLS component materials, with polymorphic structures of the component crystals and the mixed crystals forming a tight relationship.

Structural model of the solid-solution phases of the α and γ forms and the eutectic phase of the γ and β′ or β_2 forms are illustrated in Figure 7. As for α and γ forms, the SOS/SLS mixtures formed solid-solution phases in all concentration ranges because of the similarities in their thermal and structural properties (Table 1). As shown in Figure 7A, the α form of the SOS/SLS mixture is stacked in a double chain-length structure in which the stearoyl and unsaturated (oleoyl and linoleoyl) chains are packed in the same leaflets. Further thermodynamic equilibration induces a transformation from the double chain-length α form to the triple chain-length γ form. In this transformation, chain segregation occurs during the α to γ transformation in the solid state, since the steric hindrance between the stearoyl and linoleoyl chains is limited. In the γ form, the stearoyl and unsaturated (oleoyl and stearoyl) chains are packed in different leaflets (Fig. 7B). Owing to olefinic interactions between oleoyl and linoleoyl chains, coexistence between the oleoyl and linoleoyl chains in the oleic/linoleic acid leaflet occurs in the γ form having a triple chain-length structure. This interaction makes the γ form the most stable polymorph of the SOS/SLS mixture, and the transformation from γ to β′ or β_2 forms does not occur in the mixture during simple cooling and heating processes.

The structural properties of the β′ and β forms are summarized in the following: An orthorhombic perpendicular subcell is formed and FA chains are inclined by about 72° in the β′ form, whereas a triclinic parallel subcell is present and the chains are inclined by about 52° in the β form (Fig. 7C) (15). By contrast, the γ form has a parallel-type subcell for the saturated chains and a nonspecific subcell for the unsaturated chains (29). In particular, SLS is the most stable in the γ form because the linoleoyl chain leaflet is stabilized in the triple chain-length structure (32,36). Taking these structural properties into consideration, one may assume that the disordered conformation of the linoleoyl chains of the SLS fraction may cause the SOS fraction not to separate from the solid-solution phase and to transform into β′ and β_2 forms when the SLS concentration in the mixture exceeds 30%. However, when the concentration of SLS fraction is lower than about 30%, the above molecular interactions may not play a dominant role, and β′ and β_2 forms of the SOS fraction are separated from the binary mixture during α- and γ-melt-mediated transformation.

The detailed molecular interactions operative between SOS and SLS are open to future studies. Elucidation of precise

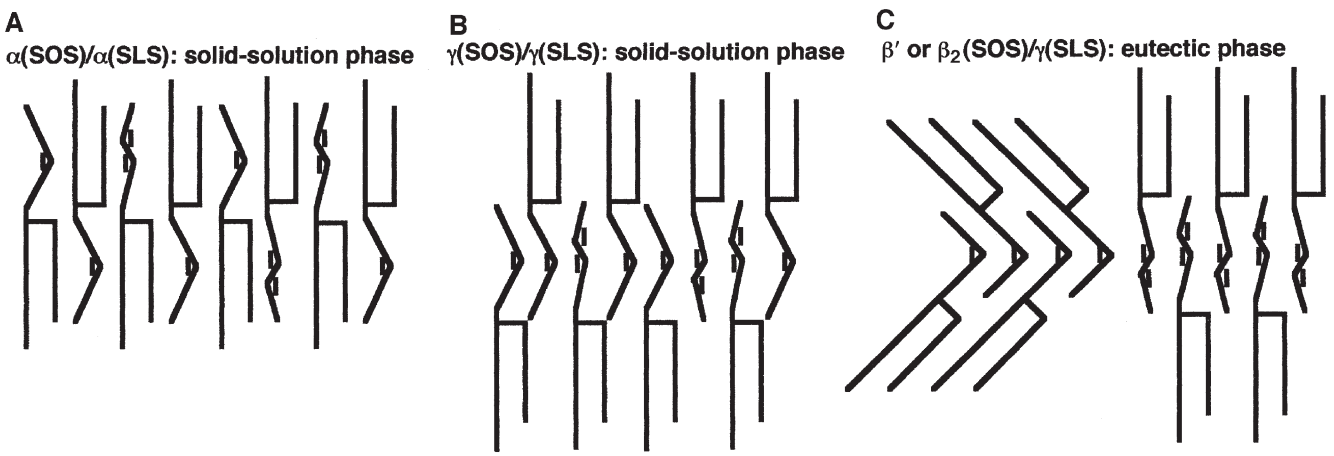

FIG. 7. Structural models of the polymorphic forms of SOS/SLS mixtures. See Figure 1 for abbreviations.

subcell packing and conformation, configuration of the olefinic group, glycerol structures, and methyl end packing would be of interest.

To summarize, separation of the SOS and SLS fractions does not occur by simple cooling at all concentration ranges. Instead, a rapid temperature increase after the cooling process can cause a separation of the SOS fraction from the SOS/SLS mixture at SLS concentrations lower than 30%. This result is, however, indicative of the process of fat blending and fat separation of SOS and SLS in the predominant heating or cooling process.

REFERENCES

1. Sato, K., Polymorphism of Pure Triacylglycerols and Natural Fats, in *Advances in Applied Lipid Research*, edited by F. Padley, JAI Press, New York, 1996, Vol. 2, pp. 213–268.
2. Padley, F.B., Chocolate and Confectionery Fats, in *Lipid Technologies and Applications*, edited by F.D. Gunstone and F.B. Padley, Marcel Dekker, New York, 1997, pp. 391–432.
3. Marangoni, A.G., and R.W. Lencki, Ternary Phase Behavior of Milk Fat Fractions, *J. Agric. Food Chem. 46*:3879–3884 (1998).
4. Blaurock, A.E., Fundamental Understanding of the Crystallization of Oils and Fats, in *Physical Properties of Fats, Oils, and Emulsifiers*, edited by N. Widlak, AOCS Press, 1999, pp. 1–32.
5. deMan, J.M., Relationship Among Chemical, Physical, and Textural Properties of Fats, *Ibid.,* pp. 79–95.
6. Dimick, P.S., Compositional Effect on Crystallization of Cocoa Butter, *Ibid.,* pp. 140–163.
7. Sato, K., and S. Ueno, Molecular Interactions and Phase Behavior of Polymorphic Fats, in *Crystallization Processes in Fats and Lipid Systems*, edited by N. Garti, and K. Sato, Marcel Dekker, New York, 2001, pp. 177–209.
8. Walstra, P., W. Kloek, and T. van Vliet, Fat Crystal Networks, *Ibid.,* pp. 289–328.
9. Small, D.M., Glycerides, in *The Physical Chemistry of Lipids*, Plenum Press, New York, 1986, pp. 345–394.
10. Moran, D.P.J., Phase Behavior of Some Palmito-oleo Triglyceride Systems, *J. Appl. Chem. 13*:91–100 (1963).
11. Wille, R.L., and E.S. Lutton, Polymorphism of Cocoa Butter, *J. Am. Oil Chem. Soc. 43*:491–4963 (1966).
12. Rossel, J.B., Phase Diagrams of Triglyceride Systems, *Adv. Lipid Res. 5*:353–408 (1967).
13. Knoester, M., P. De Bruijne, and M. Van Den Tempel, The Solid–Liquid Equilibrium of Binary Mixtures of Triglycerides with Palmitic and Stearic Chains, *Chem. Phys. Lipids 9*:309–319 (1972).
14. Timms, R.E., Phase Behavior of Fats and Their Mixtures, *Prog. Lipid Res. 23*:1–38 (1984).
15. Lutton, E.S., Phase Behavior of Triglyceride Mixtures Involving Primarily Tristearin, 2-Oleoyldistearin, and Triolein, *J. Am. Oil Chem. Soc. 32*:49–53 (1955).
16. Kerridge, R., Melting-Point Diagrams for Binary Triglyceride Systems, *J. Chem. Soc.*:4577–4579 (1952).
17. Kellens, M., W. Meeussen, A. Hammersley, and H. Reynaers, Synchrotron Radiation Investigations of the Polymorphic Transitions in Saturated Monoacid Triglycerides. Part 2: Polymorphism Study of a 50:50 Mixture of Tripalmitin and Tristearin During Crystallization and Melting, *Chem. Phys. Lipids 58*:145–158 (1991).
18. Minato, A., S. Ueno, J. Yano, Z.H. Wang, H. Seto, Y. Amemiya, and K. Sato, Synchrotron Radiation X-ray Diffraction Study on Phase Behavior of PPP–POP Binary Mixtures, *J. Am. Oil Chem. Soc. 73*:1567–1572 (1996).
19. Minato, A., Physical Study on Molecular Interactions and Phase Behavior of Binary Mixtures of Triacylglycerols, Doctoral Thesis, Hiroshima University, 1997.
20. Engstrom, L., Triglyceride Systems Forming Molecular Compounds, *J. Fat Sci. Technol. 94*:173–181 (1992).
21. Koyano, T., I. Hachiya, and K. Sato, Phase Behavior of Mixed Systems of SOS and OSO, *J. Phys. Chem. B 96*:10514–10520 (1992).
22. Minato, A., S. Ueno, K. Smith, Y. Amemiya, and K. Sato, A Thermodynamic and Kinetic Study on Phase Behavior of Binary Mixtures of POP and PPO Forming Molecular Compound Systems, *J. Phys. Chem. B 101*:3498–3505 (1997).
23. Minato, A., J. Yano, S. Ueno, K. Smith, and K. Sato, An FT-IR Study on Microscopic Structures and Conformations of POP–PPO and POP–OPO Molecular Compounds, *Chem. Phys. Lipids 88*:63–71 (1997).
24. Minato, A., S. Ueno, J. Yano, K. Smith, H. Seto, Y. Amemiya, and K. Sato, Thermal and Structural Properties of *sn*-1,3-Dipalmitoyl-2-oleoylglycerol and *sn*-1,3-Dioleoyl-2-palmitoylglycerol Binary Mixtures Examined with Synchrotron Radiation X-Ray Diffraction, *J. Am. Oil Chem. Soc. 74*:1213–1220 (1997).
25. Yano, J., and K. Sato, FT-IR Studies on Polymorphism of Fats: Molecular Structures and Interactions, *Food Res. Int. 32*:249–259 (1999).
26. Sato, K., S. Ueno, and J. Yano, Molecular Interactions and Kinetic Properties of Fats, *Prog. Lipid Res. 38*:91–116 (1999).
27. List, G.R., T.L. Mounts, F. Orthoefer, and W.E. Neff, Potential Margarines Oils from Genetically Modified Soybeans, *J. Am. Oil Chem. Soc. 73*: 729–732, (1996).
28. List, G.R., T.L. Mounts, F. Orthoefer, and W.E. Neff, Effect of Interesterification on the Structure and Physical Properties of High-Stearic Acid Soybean Oils, *Ibid. 74*:327–329 (1997).
29. Sato, K., T. Arishima, Z.H. Wang, K. Ojima, N. Sagi, and H. Mori, Polymorphism of POP and SOS. I. Occurrence and Polymorphic Transformation, *Ibid. 66*:664–674 (1989).
30. Yano, J., S. Ueno, and K. Sato, An FT-IR Study of Polymorphic Transformations in SOS, POP, and POS, *J. Phys. Chem. 97*:12967–12973 (1993).
31. Yano, J., K. Sato, F. Kaneko, D.M. Small, and D.R. Kodali, Structural Analyses of Polymorphic Transitions of *sn*-1,3-Distearoyl-2-oleoylglycerol (SOS) and *sn*-1,3-Dioleoyl-2-stearylglycerol (OSO): Assessment on Steric Hindrance of Unsaturated and Saturated Acyl Chain Interactions, *J. Lipid Res. 40*:140–151 (1999).
32. Takeuchi, M., S. Ueno, J. Yano, E. Flöter, and K. Sato, Polymorphic Transformation of 1,3-Distearoyl-*sn*-2-linoleoyl-glycerol, *J. Am. Oil Chem. Soc. 77*:1243–1249 (2000).
33. Koyano, T., I. Hachiya, T. Arishima, K. Sato, and N. Sagi, Polymorphism of POP and SOS. II. Kinetics of Melt Crystallization, *Ibid. 66*:675–679 (1989).
34. Ueno, S., A. Minato, and K. Sato, Synchrotron Radiation X-ray Diffraction Study of Liquid Crystal Formation and Polymorphic Crystallization of SOS (*sn*-1,3-distearoyl-2-oleoyl glycerol), *J. Phys. Chem. B 101*:6847–6854 (1997).
35. Ueno, S., A. Minato, J. Yano, and K. Sato, A Synchrotron Radiation X-ray Diffraction Study of Polymorphic Crystallization of SOS from Liquid Phase, *J. Cryst. Growth 198/199*:1326–1329 (1999).
36. Sato, K., Molecular Aspects in Fat Polymorphism, in *Crystallization and Solidification Properties of Lipids*, edited by N. Widlak, R. Hartel, and S. Narine, AOCS Press, 2001, pp. 1–16.

[Received September 24, 2001; accepted March 29, 2002]